SLAC-PUB-8488
June 2000

RADIATION STUDIES FOR THE ENVIRONMENTAL PROTECTION AT THE BEAM DELIVERY SYSTEM OF THE NEXT LINEAR COLLIDER*

S.H. Rokni, J. C. Liu, S. Roesler
Stanford Linear Accelerator Center
Stanford, CA 94309, U.S.A.

Abstract

The concentration of induced radionuclides in the soil and groundwater around, and air inside the collimation section of the Beam Delivery System of the Next Linear Collider are calculated with the FLUKA Monte Carlo code. The concentration of ^{3}H and ^{22}Na in groundwater are comparable to the drinking water limits. The fluence of particles (photon, neutron, proton and pion) in the air inside the tunnel for the collimation section is also calculated with FLUKA. The induced activities of ^{3}H, ^{7}Be, ^{11}C, ^{13}N, ^{15}O, and ^{41}Ar are then estimated by folding the particle fluences with various nuclear cross sections. The worker exposure during access after accelerator shutdown and the general public dose from radioactivity released to the environment are studied. The concern is from the short-lived radioisotopes of ^{13}N and ^{15}O, produced mainly by photons, and ^{41}Ar produced by thermal neutrons. The results show that the radiological consequences from the air activation are minor.

Presented at the 5Th Specialists Meeting on Shielding Aspects of Accelerators, Targets and Irradiation Facilities, SATIF 5- Paris, France, July 18-21, 2000

*Work supported by Department of Energy contract DE-AC03-76SF00515

Introduction

The collimation section of the Beam Delivery System (BDS) for the Next Linear Collider (NLC) [1] eliminates particles at large amplitude that could cause unacceptable levels of background in the detector. The collimation section consists of a series of spoilers and absorbers that are designed to absorb continuously 0.1% (10 kW) of the total beam power. Calculation of the amount of induced radioactivity in the soil that could leach out and eventually reach the public drinking water supplies is an important factor in the design of shielding for the BDS. Studies have shown that only ^{3}H and ^{22}Na could contribute significantly to the activity in groundwater and need to be considered [2,3]. Other radionuclides either have very short half-lives or are strongly absorbed in the soil (e.g. ^{7}Be, ^{45}Ca, ^{54}Mn).

Another significant factor in the design of shielding for the BDS is the amount of radionuclides produced in the air inside the tunnel for the collimation section. The airborne radionuclides in the tunnel could constitute a radiological hazard for workers accessing the tunnel after a shutdown. Additionally, if the radionuclides are released to the environment the general public may receive dose from various pathways.This paper summarizes the results from various methods used in the calculation of the induced activity of several radionuclides in the soil and gives the initial estimates for the concentration of ^{3}H and ^{22}Na in the groundwater around the collimation section of the BDS. The induced radioactivity in air inside the tunnel is also calculated; the radiological consequences from the air activation are presented. A detailed discussion of the methods used in calculating the soil, groundwater and air activation is given elsewhere [4,5].

The FLUKA Calculations

The calculations were performed using the 99 version of the Monte Carlo particle interaction and transport code FLUKA [6]. The program is used to simulate the electromagnetic and hadronic particle cascades in the beam line components, walls and soil around, and air inside the BDS tunnel. In the following sections some aspects of the simulations that are relevant to the present study are discussed.

The Geometry and Materials

A cylindrical concrete shell (inner radius=100 cm, outer radius=130 cm) surrounded by a 100-cm-thick cylindrical layer of soil (Fig. 1) was used to approximate the 300-meter long tunnel for the BDS. The collimation region is comprised of six sections, each one having two spoilers (vertical/horizontal) and two absorbers (horizontal/vertical). Each spoiler (inner radius=0.0061 cm, length=0.357 cm) is followed by an absorber (inner radius=0.05 cm, length=50 cm) located 2200 cm down-beam that is protecting a (focusing/de-focusing) quadrupole magnet (inner radius=0.7 cm, length=100 cm) that is located 50 cm down-beam of the absorber. In the FLUKA geometry, spoilers and absorbers were assumed to consist entirely of copper and magnets were made of iron. The beam pipe is a cylindrical shell made of iron (inner radius=0.5 cm, outer radius=0.6 cm). The outer radii of the spoilers, the absorbers and the magnets are all 10 cm. For soil, density=2.1 g cm^{-3}, the following chemical composition and mass fractions are used: O (54.6%), Si (30.7%), Al (4.2%), K (2.5%), Fe (1.8%), Mg (1.7%), H (1.6%), Na (1.3%), Ca (1.2%), Mn (0.003%). The water content of the soil is assumed to be 30% by volume. Air fills the rest of the tunnel.

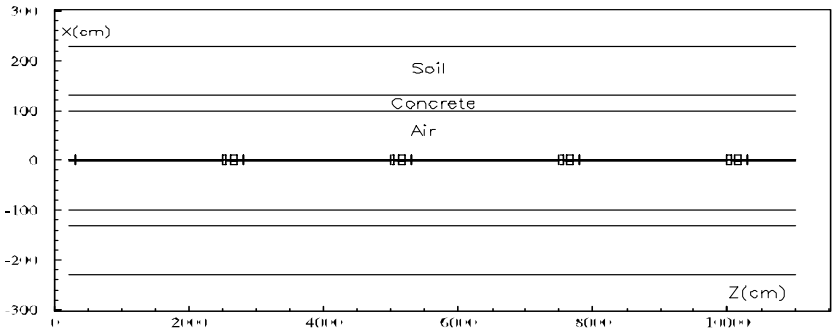

Fig. 1. Cross section of the tunnel for the collimation section of the NLC Beam Delivery System.

The lower kinetic energy transport cut-offs for electrons/positrons and for photons were all set at 5 MeV. Neutrons were transported down to the lowest thermal group of the 72 energy-group neutron cross-section of the ENEA data set. The transport threshold for all other hadrons was set to be 10 keV. The threshold for scoring the hadron inelastic reactions was set at 50 MeV. The interaction length for nuclear inelastic interactions of photons was reduced by a factor of 50 in all materials to increase photo-hadron production. Full leading particle biasing was activated for all electromagnetic processes for photons, electrons and positrons below 500 GeV in all regions. The region importance biasing for neutrons was activated in concrete and soil. The magnetic field option in FLUKA was used to set a field gradient of 9.56 kG/cm for focusing and de-focusing quadrupole magnets. The incident beam was assumed to have a δ-function size and to strike the first vertical spoiler at x=0.0066, y=0.0 and z=299.99 parallel to the z-axis.

Calculated Quantities

Three approaches using FLUKA were considered to estimate the induced radioactivity in the soil. The first approach was to estimate the radionuclide production by folding the FLUKA-calculated neutron fluence with the appropriate nuclear cross sections. The second method was to calculate directly with FLUKA the production of residual-nuclei in the soil. The third approach was to calculate the number of stars, then converting it to the number of radionuclides in soil using appropriate atom per star factors. These approaches are compared with each other by calculating the induced activity in a small region of soil with each method. This region (inner radius = 130 cm, outer radius=140 cm, length = 50 cm, starting at z=5000 cm) is across the absorber that intercepts most of the scattered beam, thus good statistical significance of the results is expected. The approaches considered in the present study are described further in the rest of this section.

Method 1-The number of atoms of ^{3}H, ^{7}Be and ^{22}Na per gram of soil per primary electron was obtained by folding the FLUKA calculated neutron fluence (see Fig. 2a) in the small region of soil with the nuclear cross sections for production of these isotopes from oxygen and silicon nuclei. Since the tunnel is shielded with a 30-cm thick concrete layer the activation of the soil outside this shield is mainly due to neutron interactions with its constituents, oxygen and silicon [7,8]. Measured cross sections for the ^{16}O(n,x)^{3}H and ^{28}Si(n,x)^{3}H reactions are not available, thus the results from an evaluation of the existing cross sections for the proton-induced reactions by Tesch [7] (see Fig. 2b) were substituted for

the unavailable neutron-induced cross sections. Therefore, results obtained with this method could have large uncertainties associated with them.

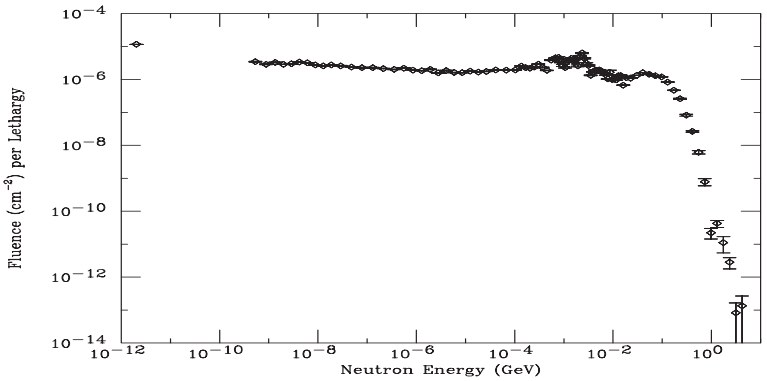

Fig. 2a. Neutron fluence in the small scoring region in the soil.

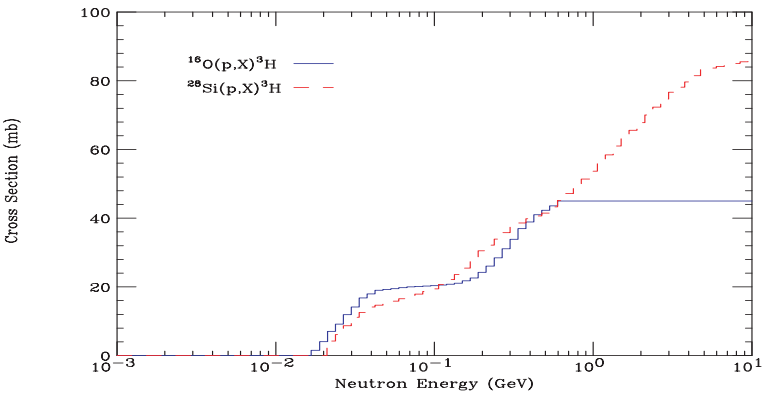

Fig. 2b. Cross sections used to calculate ^{3}H production from silicon and oxygen [7].

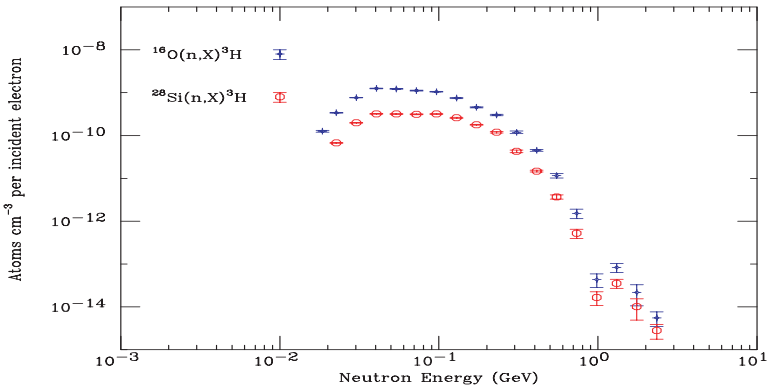

Fig. 2c. Contribution of oxygen and silicon to the activity of ^{3}H in soil.

Results of ^{3}H activity in the soil from folding of the neutron fluence spectrum with the above cross sections (Fig. 2c) show that only the spallation neutrons in the approximate energy range of 20 to 200 MeV contribute to the ^{3}H production from oxygen and silicon.

Method 2-The production of residual isotopes was directly calculated with the RESNUCLE option of FLUKA. The physics implemented in the code does not include a nuclear multi-fragmentation model, therefore the yield of nuclides with mass numbers far from the parent nuclei in medium-mass targets could be underestimated.

Method 3-Number of stars (defined as the inelastic interactions of hadrons with kinetic energies greater than 50 MeV) was calculated with FLUKA. This number was converted to the number of radionuclides using the radionuclide per star factors that can be obtained from the ratio of the measured (or calculated) activity to the calculated number of stars [9,10].

Table 1 shows the activity concentration for ^{3}H, ^{7}Be and ^{22}Na calculated by the three methods described above and for the other radionuclides calculated with methods 2 and 3 in the small scoring region in the soil. The percentage values represent the statistical uncertainty of the results. For the column labeled "Star Method", the values of atom per star from Vincke et al. [11] have been used. Note that for ^{7}Be, ^{22}Na and ^{54}Mn, these values are based on measurements on molasse.

The BDS Soil Activation

The average induced activity over the entire 300-meter-long, 100-cm-thick soil layer (volume = 3.39×10^{9} cm^{3}) that surrounds the collimation section of the BDS was then calculated by multiplying number of stars calculated with FLUKA in this region ($1.10 \pm 0.2\%$) with the appropriate radionuclide per star factors. These factors are the ratios of the number of different isotopes in the small scoring region, calculated with the RESNUCLE option in FLUKA, over the number of stars in the same region. Calculation of activity using the direct production of residual nuclei in the entire volume of soil around the BDS is much more CPU intensive than calculating the star density.

Table 1: Comparison of radionuclide production rate (atoms cm^{-3} per incident electron) in the small scoring region in soil (volume = 4.2×10^{5} cm^{3}) calculated with different methods.

Nuclide	Spectrum	Direct Isotope Production	Star Method
^{3}H	2.8×10^{-9}	5.0×10^{-10} (8 %)	1.2×10^{-9}
^{7}Be	5.1×10^{-10}	1.8×10^{-10} (19 %)	4.6×10^{-10}
^{22}Na	6.1×10^{-10}	2.9×10^{-10} (6 %)	3.2×10^{-10}
^{45}Ca	-	1.1×10^{-9} (13 %)	2.7×10^{-10}
^{54}Mn	-	1.5×10^{-10} (22 %)	1.7×10^{-10}
^{56}Fe	-	4.1×10^{-9} (22 %)	8.9×10^{-10}

Assuming that 0.1% of the beam intensity (1.25×10^{11} electrons/second) is lost on the first spoiler the average activity concentration for different radionuclides was calculated. Table 2 shows the activation for various nuclei after 10 years of NLC operation (6000 hours of continuous operation followed by 2760 hours of down-time) and 4 different cool-off periods. The natural activity concentration of the soil varies from 0.3 to 1 Bq gm^{-1}, much smaller than the total induced activity immediately after the shut-down. However, this value is dominated by ^{24}Na that has a 15 hour half-life and decays away in less than a week. Ten years after shut down the total induced activity is close to the natural background with only ^{3}H, ^{22}Na and ^{55}Fe contributing to the soil activity. With 50 years of cool-off, the total induced activity in the soil is much less than the natural activity of the soil. Additionally, some of the radionuclides (e.g. ^{3}H) could leach out of the soil and add to the activity of groundwater, thus the activity remaining in the soil would be reduced even further. It should be pointed out that currently there are no limits for soil activation in the federal, state or local government regulations in the U.S.

Table 2: Average induced activity in the soil around the BDS tunnel.

Nuclide	Half-Life	Activity Concentration (Bq gm^{-1})				
		Saturation	Shut-down	1 year	10 years	50 years
^{3}H	12.3 y	0.25	0.07	0.07	4.2×10^{-2}	4.5×10^{-3}
^{7}Be	53.3 d	0.09	0.09	-	-	-
^{22}Na	2.6 y	0.14	0.10	0.07	6.6×10^{-3}	1.6×10^{-7}
^{24}Na	15.0 h	9.37	9.37	-	-	-
^{45}Ca	163.8 d	0.55	0.45	0.10	8.9×10^{-8}	-
^{54}Mn	312.1 d	0.08	0.06	0.03	1.7×10^{-5}	1.5×10^{-19}
^{55}Fe	2.7 y	2.05	1.34	1.04	1.1×10^{-1}	4.1×10^{-6}
Activity Concentration		12.53	11.48	1.31	1.5×10^{-1}	4.5×10^{-3}

Groundwater Activation

The concern from activity in groundwater is mainly due to ^{3}H and ^{22}Na [2,3,7,8]. Here, it is assumed that 100% of ^{3}H and 15% of ^{22}Na is leached out of the soil [7,8] and is dissolved in the groundwater. After 10 years of NLC operation the activities of these two radionuclides will be 0.52 Bq cm^{-3} and 0.10 Bq cm^{-3}, respectively. It is unlikely that there will be drinking water wells close to the NLC tunnel. However, should that be the case, the calculated tritium concentration is comparable to the Environmental Protection Agency (EPA) standard for the tritium concentration in drinking water [12], 0.74 Bq cm^{-3}. The calculated concentration level for ^{22}Na in water outside the BDS is below the Department of Energy (DOE) Derived Concentration Guide of 0.37 Bq cm^{-3} [13]. With the inclusion of dilution factors and accounting for residence time of water near the collimation section the concentration of the induced activity in groundwater would be reduced to levels well below these limits. The total activity of ^{3}H and ^{22}Na in the water (1.0×10^{9} cm^{3}) outside the entire BDS is 0.6 GBq at the shut-down which is far lower than the 185 GBq limit for release to waste water per year [14].

Air Activation

FLUKA was also used to calculate the fluence of particles (photon, neutron, proton and pion) capable of producing radionuclides in the air inside the tunnel for the collimation section of the BDS. These fluences were then folded with appropriate nuclear cross sections to estimate the number radionuclides produced in air [5]. The spectrum lethargy plot in Fig. 3a shows that in the energy range between 10 MeV and 100 MeV the photon fluence dominates over hadron fluence by 2-3 orders of magnitude. In the calculations air is assumed to have a density of 0.001225 g cm^{-3} with the following composition (weight fraction): nitrogen (75.58%), oxygen (23.17%), and argon (1.25%).

The radionuclides ^{13}N and ^{15}O are produced predominantly in the giant resonance reactions, and ^{11}C, ^{3}H and ^{7}Be in photon and hadron-induced spallation reactions on nitrogen and oxygen atoms in air. Additionally, ^{41}Ar is produced in the $^{40}Ar(n,\gamma)^{41}Ar$ reaction with a cross section of 550 mb for thermal neutrons. For the giant resonance reactions of $^{14}N(\gamma,n)^{13}N$ and $^{16}O(\gamma,n)^{15}O$, the evaluation of the measured cross sections by Fasso et al. [15], and for the photo-spallation reactions of $^{16}O(\gamma,x)^{11}C$, $^{16}O(\gamma,x)^{3}H$, and $^{16}O(\gamma,x)^{7}Be$ the evaluation of the measured cross sections by Tesch [16] were used. For hadron induced reactions (e.g. $^{16}O(n,x)^{3}H$, $^{16}O(n,x)^{7}Be$) the cross sections evaluated by Huhtinen [17] using FLUKA95 were used. This was in part due to the lack of measured cross sections for the neutron-induced reactions.

Fig. 3b compares the nuclear cross sections of ^{16}O and ^{14}N for neutron and photon leading to ^{15}O or ^{13}N. The giant resonant reactions of $^{14}N(\gamma,n)^{13}N$ and $^{16}O(\gamma,n)^{15}O$ have maximum cross sections up to 15 mb peaked at ~20 MeV. Since the photon and neutron cross sections are comparable in this case, the photon component is expected to dominate the production of ^{13}N and ^{15}O completely and the contribution of hadrons is negligible. On the other hand, nuclear cross sections for production of ^{11}C from ^{16}O and ^{14}N are dominated by hadron induced reactions. However, due to the much higher fluence of photons, production of ^{11}C from oxygen and nitrogen is mainly due to photo-spallation reaction in the energy range from 30 MeV to 100 MeV. In Fig. 3c the neutron cross sections for ^{16}O leading to ^{3}H or ^{7}Be are shown. Again, due to much higher fluence, photons are the major contributor to the production of ^{3}H and ^{7}Be in air. However, the hadron contribution to the total yield is not negligible in this case (e.g., 45% for ^{3}H) [5]. The yields of radionuclides in air (atom/beam particle) inside the tunnel for the collimation section of the NLC BDS are listed in Table 3.

Worker Exposure during Access

The worker exposure during access after the accelerator shutdown was estimated based on the assumption that 1.25×10^{11} electrons per second are lost on the first spoiler. In Table 3, the activity concentration in air inside the collimation section (A_c) at the end of one-month-long operation are compared with the DAC (Derived Air Concentration) values [18]. Note that dose from exposure of 2000 DAC-h is 0.05 Sv. For these calculations it has been assumed that each access would follow one month of continuous operation with no ventilation during the operation or shut-down. The ratios of A_c / DAC for ^{13}N, ^{15}N and ^{41}Ar are higher than 1. However, a waiting period of one hour before access would reduce most activity concentrations to minimal levels. In that case only the concentration for the ^{41}Ar would exceed its DAC value.

Table 3. Worker dose estimation from air activation in the collimation section of the NLC BDS tunnel (volume = 9.4×10^8 cm^3).

Radionuclide	^{11}C	^{13}N	^{15}O	^{41}Ar	^{3}H	^{7}Be
Half-Life	20.4 min	10 min	2 min	1.83 h	12.3 y	53.3 day
Atom/Beam Particle	0.0010	0.016	0.0028	0.0018	0.00077	0.00016
A_c (Bq cm^{-3})	0.14	2.1	0.37	0.24	0.00048	0.0068
DAC (Bq cm^{-3})	0.148	0.148	0.148	0.111	0.740	0.296
A_c / DAC	0.94	14	2.5	2.1	0.00065	0.023
A_c/DAC after 1 h	0.12	0.22	0.000	1.5	0.0006	0.02

Effluent Dose to General Public

To estimate the dose to the general public from radioactivity released to the environment it is assumed that, in contrast to the previous section, the total activity in the tunnel is vented out immediately after a shut-down. Therefore, the annual activity released for each type of radionuclide (A_y) is 12 times the activity at the end of one-month-long operation. The airborne effluent dose to the public per unit activity released as a function of distance (50 m to 10 km) from the release point was calculated using the DOE-certified CAP88 computer code [19]. SLAC specific parameters and NRC (Nuclear Regulatory Commission) terrestrial food chain model parameters were used in place of the yet unknown NLC location specific parameters.

Table 4 shows that the annual dose to the Maximum Exposed Individual (Hmei) is dominated by ^{13}N, 1.9 μSv/y. The dose to the MEI, which in this case is an individual who lives 50 m from the release point, is much less than the NESHAPS [20] legal limit of 100 μSv/y. However, it is required by EPA [18] to have a continuous radioactivity monitoring system for air emission if the dose to MEI is more than 1 μSv/y. A holding period of 1 hour before air release would reduce the dose significantly such that the maximum annual dose is 0.25 μSv/y, caused mainly by ^{41}Ar. Note that the dose to general public is proportional to the activity released annually. Therefore, if the tunnel is not sealed during the operation, the actual dose could be much higher.

Table 4. Effluent dose estimation from air activation in the collimation section of the BDS tunnel.

Radionuclide	^{11}C	^{13}N	^{15}O	^{41}Ar	^{3}H	^{7}Be
Half-Life	20.4 min	10 min	2 min	1.83 h	12.3 y	53.3 day
A_y (MBq/y)	1568	24000	4200	2700	5.4	76
H_{mei} / A_y (pSv / MBq)	84	78	68	103	75	581
H_{mei} (μSv/y)	0.1	1.9	0.3	0.3	0.0004	0.04
H_{mei} (μSv/y), Hold 1 h	0.02	0.03	0.000	0.25	0.0004	0.04

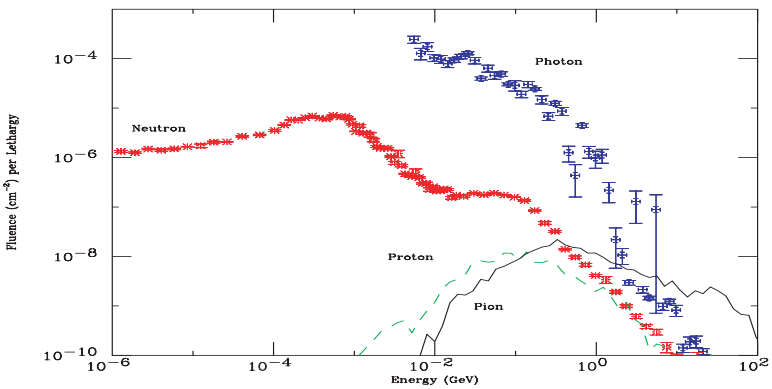

Fig. 3a. Particle fluence spectra in the NLC BDS tunnel air region [5].

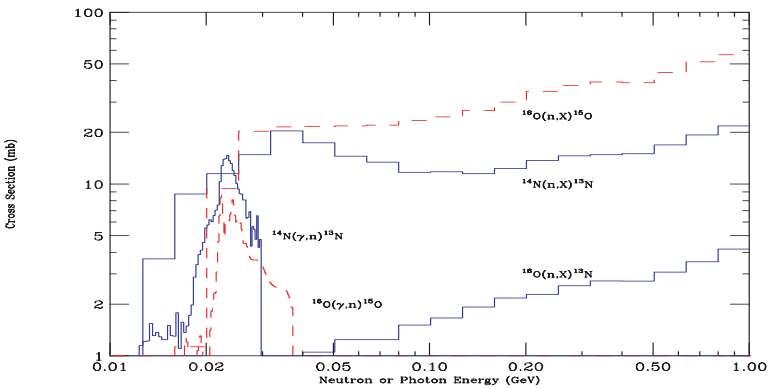

Fig. 3b. Nuclear cross sections of ^{16}O and ^{14}N for neutron and photon leading to ^{15}O or ^{13}N [5].

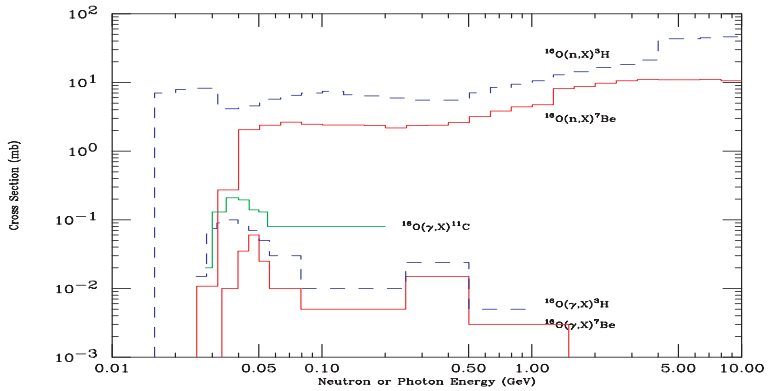

Fig. 3c. Nuclear cross sections for ^{3}H or ^{7}Be production by neutrons and photons on ^{16}O. The reaction ^{16}O(γ,x) ^{11}C is also shown for comparison [5].

Conclusions

FLUKA has been used to estimate the concentration of induced activity in the soil and groundwater around, and air inside the collimation section of the NLC Beam Delivery System. Different methods are used to calculate the activity concentrations for ^{3}H, ^{7}Be and ^{22}Na in the soil. Following 10 years of NLC operation, the activity concentration in the soil drops to the same level as the natural background after a 10 year cool-off period. The activity concentration for ^{3}H and ^{22}Na in groundwater are also estimated. After 10 years of operation, the concentration levels for ^{3}H is below the EPA drinking water limit. Dilution factors, not considered here, are expected to lower the concentration levels significantly below the applicable EPA and DOE limits. The total activity in groundwater from this section of the NLC is far below the limit for release to waste water.

The FLUKA calculations also show that the photon fluence dominates the radioactivity production in the air due to its much higher intensity than hadrons. Photons with energy between 10 and 100 MeV are contributing most to the production of ^{3}H, ^{7}Be, ^{11}C, ^{13}N, ^{15}O in air. However, for ^{41}Ar, it is the thermal neutron component that dominates the activation. The worker exposure during access after one month of operation is not a major concern (dose dominated by the short-lived radioisotopes of ^{13}N, ^{15}O, and ^{41}Ar), and if desired can be easily mitigated by waiting for one hour before access. Assuming that all radioactivity in the air at the end of one-month-long operation is released to a meteorological and ecological environment that is same as that of SLAC, the annual dose to the general public was found to be minor (again the dose comes from ^{13}N, ^{15}O, and ^{41}Ar). The hazard can be mitigated by means of decay (e.g., wait one hour prior to the release) and in that case the hazard will be mainly due to ^{41}Ar.

Acknowledgements

We wish to thank the authors of FLUKA for making the code available to us, and would like to acknowledge helpful discussions with A. Fasso, and L. Keller

References

1. NLC Design Group, “Zeroth-Order Design Report for the Next Linear Collider”. SLAC Report 474 (LBNL-PUB-5424), 1996.
2. T.B. Borak, M. Awschalom, W. Fairman, F. Iwami, J. Sedlet, “The underground migration of radionuclide produced in soil near high energy proton accelerators”, Health Phys. 23:679-687; 1972.
3. S. Baker, J. Bull, D. Gross, “Leaching of accelerator produced radionuclides”, Health Phys. 73 :912- 918;1997
4. S. Rokni, J. C. Liu and S. Roesler, “Initial estimates of the activation concentration of the soil and groundwater around the NLC Beam Delivery System tunnel”, SLAC RP Note RP-00-04, May, 2000.
5. J. C. Liu, S. Roesler, S. Rokni and R. Sit, “Evaluation of Radiological Consequence from Air Activation at NLC BDS Tunnel”, SLAC RP Note RP-00-05, May, 2000

6. A. Fasso, A. Ferrari, J. Ranft and P. R. Sala, “New developments in FLUKA modeling of hadronic and EM interactions”, Proceedings of the Third Workshop on Simulating Accelerator Radiation Environments (SARE-3), KEK, Tskuba, Japan, p.32, 1997.
7. K. Tesch, “Production of radioactive nuclides in soil and groundwater near dump of a linear collider”, DESY Internal Report-DESY, D3-86, January 1997.
8. B. Racky, H. Dinter, A. Leuschner and K. Tesch, “Radiation environment of the linear collider TESLA”, Proceedings of the Fourth Workshop on Simulating Accelerator Radiation Environments (SARE-4), Knoxville, Tennessee, U.S.A., p. 14, 1998.
9. J. Ranft, K. Goebel, “Estimation of induced radioactivity around high-energy accelerators from hadronic cascade star densities obtained from Monte Carlo calculations”, CERN HP-70-92, 1970.
10. A. H. Sullivan, “Groundwater activation around the AA and ACOL target areas”, CERN Internal Report CERN/TIS-RP/IR/87-34, 1987.
11. H. Vincke and G. R. Stevenson, “Production of radioactive isotopes in molasse”, CERN Internal Report CERN/TIS-RP/IR/99-20, 1999.
12. U.S. Environmental Protection Agency. Code of Federal Regulations. Washington D.C., U.S. Government Printing Office; 40CFR part 141. 1992.
13. U.S. Department of Energy, “Radiation Protection of the General Public and the Environment”, 10CFR834, Federal Register, 1993.
14. California Code of Regulation (CCR), Title 17, Public Health, Division 1, Chapter 5, Subchapter 4, Group 3, Article 30287 (1994).
15. A. Fasso, A. Ferrari, P.R. Sala, “Total Giant Resonance photonuclear cross sections for light nuclei: A database for the FLUKA Monte Carlo transport code”, Proceedings of the 3rd Specialists' Meeting on Shielding Aspects of Accelerators, Targets and Irradiation Facilities (SATIF 3), Tohoku University, Sendai, Japan, 12-13 May 1997, p.61, OECD-NEA, 1998.
16. K. Tesch and H. Dinter, “Production of radioactive nuclides in air inside the collider tunnel and associated doses in the environment”, DESY Internal Report DESY-D3-88, January 1998.
17. M. Huhtinen, “Determination of Cross Sections for Assessments of Air Activation at LHC”, CERN Internal Report CERN/TIS-RP/TM/96-29, 1997.
18. U.S. Department of Energy, Occupational Radiation Protection, 10CFR835, Federal Register, Final Rule, November, 1998.
19. B. Parks, CAP88 PC Code (Version 1), US Department of Energy, Germantown, MD, 1992.
20. 40CFR61, National Standards for the Emission of Radionuclides Other Than Radon from Department of Energy Facilities (NESHAPS), Code of Federal Regulation, Subpart H, 1989.